

## RMP ELM CONTROL UNVEILS HIGH ION TEMPERATURE WITH ITB IN THE DIII-D TOKAMAK

Q.M. HU<sup>1</sup>, H.Q. WANG<sup>2</sup>, X.D. DU<sup>2</sup>, S. HASKEY<sup>1</sup>, S.Y. SHI<sup>3</sup>, A. BORTOLON<sup>1</sup>, S.Y. DING<sup>2</sup>, R.J. HONG<sup>4</sup>, S.K. KIM<sup>1</sup>, N.C. LOGAN<sup>5</sup>, T. ODSTRCIL<sup>2</sup>, Z. YAN<sup>6</sup>

<sup>1</sup> Princeton Plasma Physics Laboratory, Princeton, USA

<sup>2</sup> General Atomics, San Diego, USA

<sup>3</sup> Oak Ridge Associated Universities, Oak Ridge, USA

<sup>4</sup> University of California at Los Angeles, Los Angeles, USA

<sup>5</sup> Columbia University, New York, USA

<sup>6</sup> University of Wisconsin, Madison, USA

Email: [qhu@pppl.gov](mailto:qhu@pppl.gov)

A stationary high ion temperature regime with an ion internal transport barrier (ITB) is robustly observed in the DIII-D tokamak during edge-localized modes (ELMs) control experiments utilizing resonant magnetic perturbations (RMPs). In the DIII-D ITER-similar shape (ISS), low-collisionality plasmas with moderate NBI heating (4–8 MW), the application of RMP ( $n = 1, 2$  and  $3$ ) typically induces a 20–30% density pump-out, doubling ion temperature regardless of suppression or mitigation of ELMs. This results in sustained core  $T_i$  of up to 18 keV and pedestal  $T_i$  of up to 4.5 keV for durations exceeding ten times the energy confinement time. Remarkably, this high  $T_i$  ITB is observed across a wide range of  $T_i/T_e$  ratios, from 1.5 to 5. The formation of high  $T_i$  ITB signifies advancements in plasma performance, showcasing enhanced confinement quality with  $H_{98}$  increasing from 1 to 1.6, effective impurity control ( $Z_{\text{eff}} \sim 2$ ), and resilience to variations in injected torque, and hysteresis effect to sustaining ion ITB when raising the density. These findings underscore the benefits of utilizing RMP for ELM control to achieve high confinement quality and high  $T_i$  with ITB.

DIII-D has been using RMP to control type-I ELMs for over two decades, frequently observing stationary high ion temperature regime. For example, in a representative experiment with  $H_{98} = 1.0$ ,  $q_{95} = 3.5$ ,  $\beta_N = 2.1$ , and  $\sim 7$  MW NBI heating in Fig. 1, the application of 3.2 kA  $n = 3$  RMP led to immediate density pump-out (Fig. 1c), reducing the core line-averaged density from  $3.5\text{--}4 \times 10^{19} \text{m}^{-3}$  to  $2.0\text{--}2.5 \times 10^{19} \text{m}^{-3}$ , followed by complete ELM suppression (Fig. 1a). Associated with density pump-out, core  $T_i$  increased from  $\sim 6$  keV to 18 keV over one second, sustained for duration exceeding 15–20 times the energy confinement time ( $\tau_E = 0.1$  s). Drop of the core  $T_i$  at the end of the discharges is due to the drop of heating power instead of chirping mode collapse reported in DIII-D before [1]. CER measurement shows global increase in the ion temperature (C-VI) as illustrated in Fig. 1e with  $T_{i,0} = 18$  keV,  $T_{i,\text{ped}} = 4.5$  keV and steeper gradient in the region of  $\rho = 0.2\text{--}0.5$ . TRANSP [2] analysis for the discharge (122483) shows much smaller and a well in the ion diffusivity in the steep  $T_i$  region, indicating the formation of ion ITB. Analysis of more discharges shows robust formation of ion ITB in the similar radial location.

The absence of core MHD modes (sawtooth, fishbone), and the interplay between fast ions, Alfvén eigenmodes (AEs) and ion temperature gradient (ITG) turbulence play an important role in the ion ITB formation. It is found that early heating power is essential to extend the current diffusion time and achieve higher  $q_{\text{min}}$  ( $\sim 1.5$ , Fig. 1c), which helps to avoid core fishbone and sawtooth crashes. In contrast, discharges with periodic sawtooth crash showed significantly lower  $T_{i,0}$ , never exceeding 9 keV. Associated with the density pump-out, multiple AEs appear as indicated by the spectrum of density fluctuations in Fig. 1d. The frequency of AEs continuously increases as  $T_{i,0}$  increases, then they transit to kinetic ballooning modes (KBMs) at around 3.5 s when  $q_{\text{min}}$  drops to  $\sim 1$ , leading to the saturation of  $T_{i,0}$ . The KBMs observed here—due to higher  $q_{\text{min}}$  and smaller radial extent—cause negligible reduction in  $T_{i,0}$  at later times (e.g. 4.3 s and 4.7 s), different to the significant collapses associated with coupling between core KBMs and edge modes [1]. Transport modeling using TGLF reproduces the observed  $T_i$  profile, and it identifies the absence of ITG modes, consistent with the experimental observation of ITB formation.

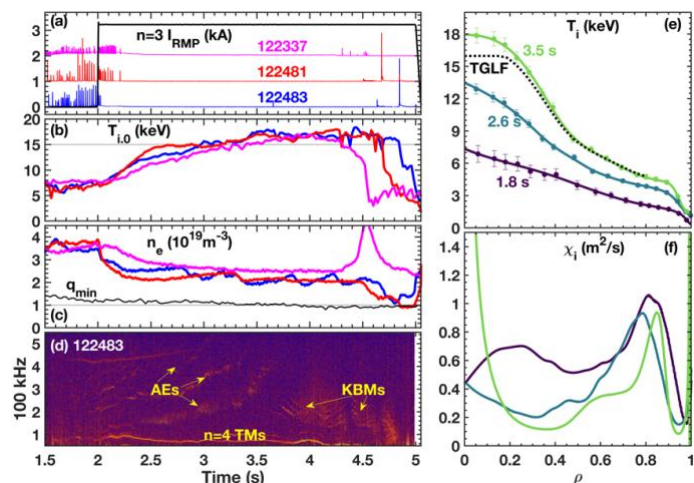


Figure 1: (a–d) Time evolution of  $D_\alpha$ , RMP coil current,  $T_{i,0}$ , core density for shots 122337, 122481 and 12483,  $q_{\text{min}}$  and spectrum of density fluctuation for shot 122483. (e)  $T_i$  profiles and (f) TRANSP calculated ion diffusivity for shot 122483. Here, TGLF calculated  $T_i$  profile at 3.5 s is shown in dotted in (e).

Ion ITB is sustained within the same density range required for accessing RMP ELM suppression. Analysis of the DIII-D RMP ELM control database over the past 20 years identifies the operational condition for achieving high  $T_i$  with ITB. As shown in Fig. 2a, where each data point represents a 200 ms average, ITB with  $T_{i,0} > 10$  keV can be achieved under  $n = 1, 2$  and 3 RMP when the core line-averaged density is below  $5 \times 10^{19} \text{m}^{-3}$  (or pedestal density below  $3.5 \times 10^{19} \text{m}^{-3}$ ). This density range aligns with the conditions required for RMP-driven ELM suppression [3], demonstrating the compatibility of high  $T_i$  ITB with RMP ELM control. Ion ITB is predominantly achieved with moderate NBI heating power, in the range of 4 - 8 MW. Higher heating power increases  $\beta_N$ , inducing low  $n$  MHD modes (e.g.  $m/n = 2/1$  NTMs), which degrade the ion ITB. For instance, strong density pump-out allows the sustenance of  $T_{i,0} = 12\text{-}15$  keV with 4 MW NBI heating power. Analysis of the electron and ion temperature profiles shows that ion ITB robustly formed at  $\rho = 0.2\text{-}0.5$  with  $T_{i,0}/T_{e,0}$  ratio ranging from 5 to 1.5 as illustrated in Fig. 2b.

The observed ion ITB in DIII-D demonstrates significant advancements with notable implications for future devices. First, high  $T_i$  with ITB is found to be independent of the injected torque/plasma rotation. As illustrated in Fig. 3a-3c, two discharges with similar plasma parameters—shot 128475 with 6 Nm torque and shot 128477 with 2 Nm—exhibited over threefold difference in core toroidal rotation after 3.5 s. Despite this, both discharges achieved the same  $T_{i,0} = 12$  keV, highlighting the robustness of ion ITB even under low torque injection. Second, the formation of ion ITB leads to significant improvements in plasma confinement. As shown in Fig. 3d-3g, increasing  $T_{i,0}$  and ITB formation correlate with a rise in  $H_{98}$  from 1.0 to 1.2, further improving to 1.6 as RMP current is gradually reduced and additional gas puffing. Third, unlike ELM suppression without ion ITB where  $Z_{\text{eff}}$  tends to increase to above 3,  $Z_{\text{eff}}$  remains nearly constant during these discharges, and the brightness of high-Z impurity Nickel ( $\text{Ni}^{26}$ ) keeps almost constant after 2 s. TGYRO calculations using the measured profiles indicate a balance between outward diffusion and inward pinch effects for tungsten impurity in the core region, suggesting the potential for mitigating impurity accumulation through a combination of core ITB screening and edge RMP pump-out. Fourth, the hysteresis effect observed following ion ITB formation enables the plasma density to increase while maintaining the ITB, as evidenced by the data in Fig. 3d-3g. Finally, ECH is shown to enhance ion ITB formation. As reported in [4], applying 1–1.5 MW off-axis ECH during RMP-driven ELM suppression triggers the development of a super-H pedestal and ion ITB formation, further advancing plasma performance.

In conclusion, the DIII-D experiments reveal the feasibility of achieving high ion temperatures with ITB and improved confinement quality through RMP-induced ELM control. These findings provide valuable insights for future burning plasma experiments, including ITER, by establishing a pathway to maintain reactor-relevant plasma conditions while managing impurity accumulation and maintaining operational flexibility. The results emphasize the potential of integrating RMPs and ITB mechanisms to advance the performance of fusion devices.

#### ACKNOWLEDGEMENTS

This material is based upon work supported by the Department of Energy under Award Number(s) DE-AC02-09CH11466, DE-FC02-04ER54698, DE-SC0022270 and DE-AC52-07NA27344.

#### REFERENCES

- [1] Du X., et al., Phys. Rev. Lett. **127** (2021) 025001
- [2] Breslau J., et al., TRANSP v18.2. [Computer Software](#) (2018)
- [3] Hu Q., et al., Phys. Plasmas **28** (2021) 052505
- [4] Logan N.C., et al., Nucl. Fusion **64** (2024) 014003
- [5] Hu Q., et al., Nucl. Fusion **61** (2021) 106006

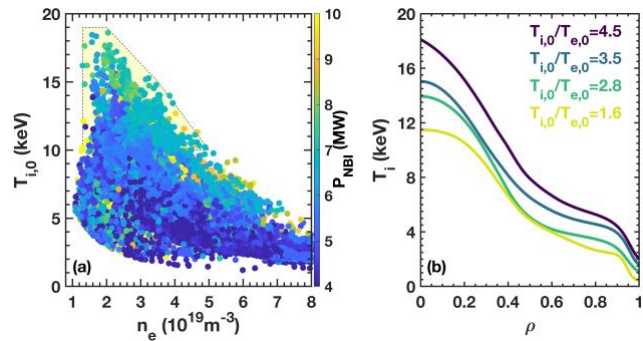


Figure 2: (a) Core  $T_i$  versus core density colored by the NBI power; (b)  $T_i$  profiles for shots with different  $T_{i,0}/T_{e,0}$ .

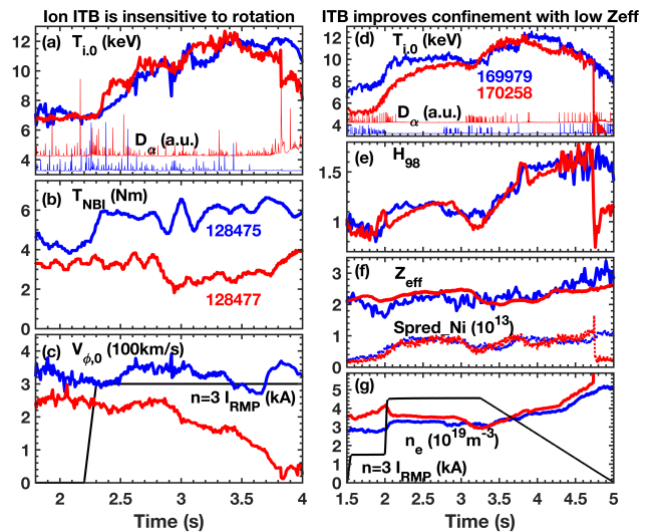


Figure 3: Time evolution of (a-c)  $T_{i,0}$ ,  $D_\alpha$ , NBI torque, core toroidal rotation and  $I_{\text{RMP}}$  for shots 128475 and 128477, (d-g)  $T_{i,0}$ ,  $D_\alpha$ ,  $H_{98}$ ,  $Z_{\text{eff}}$ , Ni impurity brightness, density and  $I_{\text{RMP}}$  for shots 168879 and 170258.